Hindawi
International Journal of Electrochemistry
Volume 2018, Article ID 8416268, 9 pages
https://doi.org/10.1155/2018/8416268

Research Article

Synthesis and Electrocatalytical Application of Hybrid Pd/Metal Oxides/MWCNTs

Yuh-Jing Chiou,[1] **Guo-Hao Wu**,[2] **Hong Ming Lin**,[2] **Andrzej Borodziński**,[3] **Piotr Kedzierzawski**,[3] **and Leszek Stobinski**[4]

[1]*Department of Chemical Engineering, Tatung University, 104 Taipei, Taiwan*
[2]*Department of Materials Engineering, Tatung University, 104 Taipei, Taiwan*
[3]*Institute of Physical Chemistry, Polish Academy of Sciences, 01-224 Warsaw, Poland*
[4]*Warsaw University of Technology, Woloska 141, 02-507 Warszawa, Poland*

Correspondence should be addressed to Yuh-Jing Chiou; ttulchiou@gmail.com

Received 26 January 2018; Accepted 8 May 2018; Published 6 June 2018

Academic Editor: Joanne Holmes

The performance of Pd electrocatalysts for formic acid electrooxidation was improved by application of metal oxide-multiwall carbon nanotubes composites as a catalyst support. Hybrid oxides/MWCNTs were synthesized by two different methods: chemical reduction method and impregnation method. Pd based catalysts were synthesized by polyol method on the MWCNTs or oxide/MWCNTs composites. The In_2O_3 was deposited on MWCNTs by impregnation method (In_2O_3/MWCNTs-IM support) and in the presence of $NaBH_4$ (In_2O_3/MWCNTs-$NaBH_4$ support). The physical properties of the Pd/In_2O_3/MWCNTs-IM, Pd/In_2O_3/MWCNTs-$NaBH_4$, Pd/SnO_2/MWCNTs, and Pd/MWCNTs catalysts were characterized and their electrocatalytical performance in formic acid oxidation was compared. During Pd deposition on In_2O_3/MWCNTs-$NaBH_4$ support, $InPd_2$ structure was formed as observed by XRD. The electrochemical tests indicate that the two Pd/ In_2O_3/MWCNTs electrocatalysts have higher electrocatalytic activity than those of Pd/SnO_2/MWCNTs and Pd/MWCNTs. The best performance was observed for the catalyst obtained by In_2O_3 impregnation of MWCNTs denoted by Pd/In_2O_3/MWCNTs-IM.

1. Introduction

Growing environmental pollution and the fact that crude oil resources are going to be exhausted stimulate an intensive development of work on replacing petroleum fuels by biofuels and by application of fuel cells for production of electricity. The application of biofuels results in reducing the emission of CO_2 and other pollutants. The content of CO_2 emitted in conversion of biofuels is equivalent to the respective content absorbed from the atmosphere by green plants in a process of biosynthesis; thus the application of biofuels as energy sources leads to overall CO_2 zero emission, what is very important for decreasing of the effects of global warming. Fuel cells are the most efficient electrical energy producing devices, operating using fuels and oxygen as reactants. Fuel cells directly transform chemical energy to electric energy with high efficiency. The most common fuels are hydrogen in proton exchange membrane fuel cells (PEMFCs), methanol in direct methanol fuel cells (DMFC), and formic acid in direct formic acid fuel cells (DFAFC). All these fuels can be produced from biomass. Fuel cells operating on liquid fuels for small and medium scale applications have prospects of commercialisation, and low temperature direct formic acid fuel cells (DFAFC) appear among the most promising in this respect [1]. DFAFC has a number of advantages over direct methanol fuel cells [1]: (i) it has higher power density and higher energy efficiency, (ii) crossover flux of formic acid through Nafion® membrane is several times smaller than that of methanol [2], and (iii) formic acid is less toxic than methanol and does not have the risk of producing hazardous by-products during oxidation (e.g., formaldehyde). A number of reviews on DFAFC [1, 3–8] have been published.

The oxidation of formic acid in DFAFC proceeds according to the following scheme:

$$\text{Anode: } HCOOH \rightarrow CO_2 + 2H^+ + 2e^-$$

Cathode: $1/2O_2 + 2H^+ + 2e^- \rightarrow H_2O$

Overall reaction: $HCOOH + 1/2O_2 \rightarrow CO_2 + H_2O$

The anode reaction proceeds by dual pathway mechanism as follows:

Pathway 1: $HCOOH \rightarrow CO_2 + 2H^+ + 2e^-$

Pathway 2: $HCOOH \rightarrow CO_{ads} + H_2O \rightarrow CO_2 + 2H^+ + 2e^-$

Pathway 2 operates on Pt electrode and pathway 1 on Pd one.

Palladium is a very effective electrooxidation catalyst formic acid; however, it works perfectly in the very pure, and so, very expensive formic acid. In a formic acid of lower purity, palladium becomes gradually poisoned, mainly, by $-CH_3$ group containing impurities [9–12], which are oxidized via adsorbed CO, blocking further reaction.

Palladium catalysts are very active in the oxidation of high purity formic acid, which is expensive. In low purity formic acid, the Pd catalysts become poisoned by CO originating from oxidation of impurities [13–15]. While some of the catalysts are poisoning resistant in the long term, their activity is still too low and developing novel electrocatalysts is still crucial for their practical applications in DFAFC. For this reason, recently, intensive research is being carried out on developing more advanced Pd based nanocatalysts in order to improve the catalyst performance.

Different approaches are applied including Pd alloying, Pd surface decoration with other elements, support modification, and catalyst morphology optimization. As alloying elements, Ru [16–18], Pt [19, 20], Ir [20–23], B [24, 25], Au [26], Sn[27], Co [28], and Bi [29] were applied. Surface of Pd nanoparticles was decorated by irreversible adsorption or underpotential deposition (UPD) of Sb, Pb, and Bi nanoclusters, which are effective for creating discontinuing Pd sites and thus hinder the CO formation (i.e., the indirect pathway) [30–32].

One of the most promising approaches, improving activity and stability of the catalysts, was modification of carbon support (carbon black, MWCNTs) with metal oxides. Among the oxides, TiO_2 [33, 34], MoO_x [35], ITO [36], ZrO_2 [37], SnO_2-TiO_2 [38], and CeO_x [39] were employed. It is expected that metal oxides will promote the oxidation of reaction poison species adsorbed on the electrode, change the electronic properties by metal-support interaction, and prevent Pd nanoparticles from sintering.

The other very efficient support modifiers employed were Ni_2P [40, 41], Co_2P [42], and conducting polymers [43]. It was also shown that the catalyst morphology optimization may lead to increasing electrochemically available surface, specific activity of the metal nanoparticles, and power density [44, 45].

In this study, nano-hybrid MOS/MWCNTs, tin oxide/MWCNTs, indium oxide/MWCNTs, and indium tin oxide/MWCNTs were prepared by impregnation method as supports for electrocatalysts. Then, Pd nanoparticles were synthesized by polyol method to deposit on the prepared MOS/MWCNTs supports. The purpose of indium oxide or tin oxide modification is to supply oxidizing centers and change the electronic properties by metal-support interaction.

Multiwalled carbon nanotubes (MWCNTs) as a substrate can make fuel cells more efficient. The main purpose of using a support is to achieve an optimal dispersion of the catalytic active component and to stabilize it against sintering. Carbon nanotubes (CNTs) are of interest as catalyst support for applying in fuel cells due to their unique electrical and structural properties [46, 47]. CNTs can both improve the effectiveness of the catalyst by altering the electron conductivity of the catalyst layer and prevent sintering of metal nanoparticles. The authors in the recent researches used MWCNTs as the support of catalysts and obtained very promising results [26, 48, 49]. However, tin and indium oxides are semiconductors with band gaps of 2.7-4.3 eV and 2.6-3.5 eV, respectively, and may brake electrical path between Pd nanoparticles and MWCNTs [49]. Indium tin oxide (ITO, or tin-doped indium oxide) is a solid solution of indium (III) oxide (In_2O_3) and tin (IV) oxide (SnO_2), typically In_2O_3:SnO_2 = 9:1 by weight%. It is one of the most widely used transparent conducting oxides because of its two chief properties, its electrical conductivity and optical transparency [50]. The adding of Sn can replace In element in the In_2O_3 lattice and form SnO_2. The forming of SnO_2 will donate one electron to the conducting band and create oxygen vacancy increasing the carrier density and so, the oxide conductivity [51]. Javier Parrondo et al. studied catalytic activities of Pt/In_2O_3/C composite catalysts with different compositions of In_2O_3 as anode catalyst for direct ethanol fuel cells (DEFCs). It was demonstrated that Pt/In_2O_3/C has higher activity towards ethanol oxidation than that of Pt/C, and the enhancement of activity could be attributed to the effects of In_2O_3 adjacent to Pt (bifunctional effect) [52].

2. Experimental

2.1. Synthesis of Hybrid Electrocatalysts. In order to prepare the nanoparticles, the following chemicals were used in this study: multiwalled carbon nanotubes (CNT Co., Ltd., Korea, 93%), nitric acid (HNO_3, Merck KGaA. Ltd., Germany, 65%), tin (II) chloride ($SnCl_2$, Wako Pure Chemical Industries, Ltd., Japan, 97.0%), indium chloride ($InCl_3$, Alfa Aesar. Ltd., England, 99.99%), hydrochloric acid (HCl, Wako Pure Chemical Industries, Ltd., Japan, 35~37%), palladium chloride ($PdCl_2$, Wako Pure Chemical Industries, Ltd., Japan, 99%), ethylene glycol (EG, Wako Pure Chemical Industries, Ltd., Japan, 99.0%), potassium hydroxide (KOH, Wako Pure Chemical Industries, Ltd., Japan, 85.0%), sodium boron-hydride ($NaBH_4$, Sigma-Aldrich Co., Ltd., United States, 98%), and citric acid (Sigma-Aldrich Co., Ltd., United States, 97%). All the synthesis flowcharts are shown in Figure 1. After the acidizing treatment, the product is denoted as AO-MWCNTs. The 20wt% metal oxides modified AO-MWCNTs (80wt%) are denoted as In_2O_3/MWCNTs and SnO_2/MWCNTs. There are two different ITO/MWCNTs prepared with indium oxide to tin oxide weight ratio as 1:1 and 9:1. In_2O_3/MWCNTs-$NaBH_4$ were synthesized by chemical reduction method (Figure 1(c)). This method is expected to form some bimetal

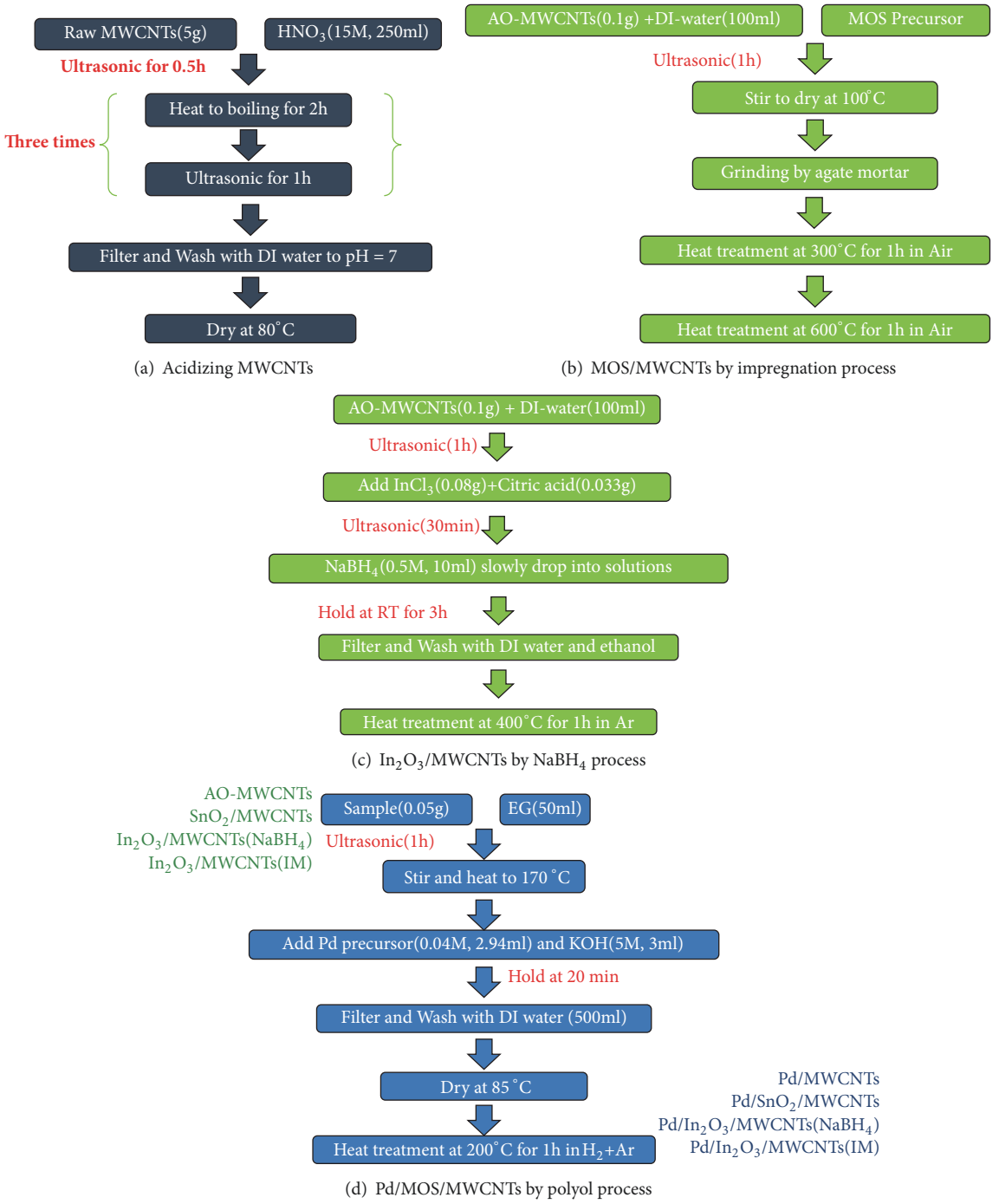

Figure 1

structure and enhance the electrocatalytic performance in DFAFC. As is shown in Figure 1, ultrasonic treatment was applied both, for MOS deposition on MWCNTs and in the initial step of Pd deposition on MOS/MWCNTs supports. For ultrasonication, the bath (Delta ultrasonic cleaner DC200H, 40kHZ, 200W) was used below 40°C. It should be emphasized that application of ultrasounds was employed for homogenization of MOS precursors and MWCNTs or Pd precursor and MOS/MWCNTs supports. Although high energy ultrasound treatment alone can lead to metal nanoparticle deposition by producing strongly reductive radicals, Nafion disintegration, and metal particle detachment from the support [53–55], we used ultrasound only for initial homogenization purposes. It should be mentioned here that highly active formic acid oxidation catalysts were already obtained [56, 57].

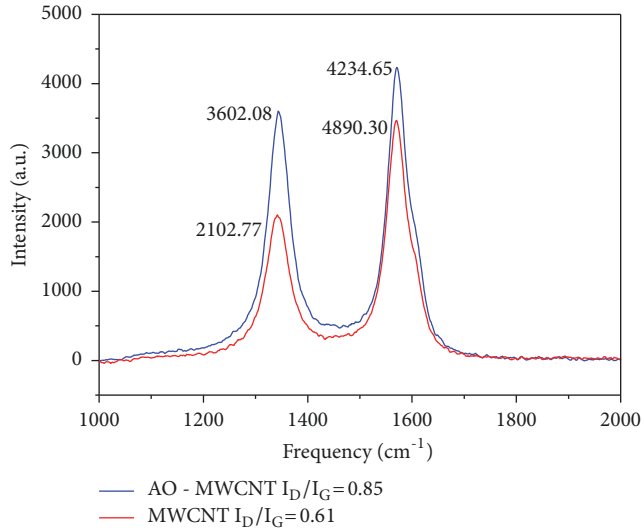

Figure 2: Raman spectra of raw MWCNTs and AO-MWCNTs.

2.2. Characterization and Electrocatalytical Performance. The acid-oxidizing degree of MWCNTs was determined by Raman spectra. The structures of the prepared samples were determined by XRD, FESEM, and HRTEM. In order to evaluate the composition of the hybrid nanoparticles, about 5mg sample was dissolved in aqua regia for 100h, and then the solutions were diluted in volumetric flask and filtered. The samples were analyzed by ICP (Perkin Elmer Optima-2000 DV) in Precise Instrument Center of Tatung University. Electrochemical activities of catalysts were characterized by C-V (cyclic voltammetry) measurement using a three-electrode cell and CHI Instrument Model 600-D potentiostat/galvanostat instrument, located in Department of Materials Engineering, Tatung University. Three-electrode cell system is composed of working electrode, Pt plate counter electrode, and a Ag/AgCl reference electrode. The electrolyte solution is a mixture of 1 M H_2SO_4 and 3 M HCOOH in equal volume at room temperature. The rotating velocity of RDE working electrode is 1600 rpm. Scan rate is 10 mV/s with scan potential range from -0.2 V to 1 V. During each C-V experiment, the dissolved gas, oxygen, CO, or CO_2 is removed from the solution by purging Argon before and during testing the cell.

3. Results and Discussion

3.1. Structure Characterization. The Raman spectra of raw MWCNTs and acid oxidized MWCNTs (AO-MWCNTs) are shown in Figure 2. Two features are observed in Raman spectra that include the disorder induced mode, the so-called D band (centered at ~1350 cm^{-1}), and the graphite mode, G band (centered at ~1589 cm^{-1}). For AO-MWCNTs, both functional groups and defects on the surface formed by the acid oxidation lead to an increase of D/G intensity ratio [20].

The XRD patterns of metal oxides modified MWCNTs and Pd electrocatalysts on various substrates are shown in Figure 3. Firstly, for In_2O_3 modified MWCNTs via impregnation and $NaBH_4$ methods, both have same structure as the commercial In_2O_3 powder. For the patterns of the prepared ITO in different SnO_2 and In_2O_3 ratios, the large peak at 26° can be identified as carbon from MWCNTs, and the other SnO_2 characteristic peaks cannot be found. The basic structure and composition analysis (Table 1) show that the prepared ITOs may not perform as expected.

For the two In_2O_3/MWCNTs prepared by two different methods, XRD patterns in (b) show the same structure as commercial indium oxide powder. After Pd depositing onto the substrates, AO-MWCNTs and the prepared MOS/MWCNTs, in (c) and (d), Pd particles were successfully synthesized. Pd/In_2O_3/MWCNTs-Impregnation, which is supported on In_2O_3/MWCNTs prepared by impregnation, still retains cubic indium oxide structure, while in In_2O_3/MWCNTs-$NaBH_4$ the In_2O_3 was partly converted to orthorhombic $InPd_2$ in reaction with Pd. There are some researches who synthesized $InPd_2$, In_3Pd_5, or $InPd_3$ by iodine catalyzed reaction from elements at 850 K [21, 22].

The FESEM and HRTEM morphology images of the hybrid nanoparticles are presented in Figure 4. By analyzing the fringe patterns of some particles in the HRTEM images, the nanoparticles can be recognized as Pd, In_2O_3, or SnO_2. All the designed compositions were in a qualitative agreement with EDS analysis. According to the FESEM images, the SnO_2 particles have the smallest particles (around 2-10 nm) comparing to other MOS particles. The MOS particles are uniformly dispersed on the surface of MWCNTs with the exception of ITO, where some large conglomerates can be also visible. The fine Pd nanoparticles (around 2-10 nm) are deposited on the surface of MWCNTs. The Pd nanoparticles formed on MOS/MWCNT composites are much larger. This is confirmed by XRD data where using Sherrer's equation, the Pd average size can be estimated at 36.8 nm and 40.3 nm for Pd/In_2O_3/MWCNTs and Pd/SnO_2/MWCNTs, respectively.

The composition of every sample, evaluated by ICP-OES analysis, is shown in Table 1. All the Pd based catalysts have

Table 1: Sample composition.

	Pd		In_2O_3		SnO_2	
	Theoretical	Experimental	Theoretical	Experimental	Theoretical	Experimental
Pd/MWCNTs	20wt%	18.66wt%				
ITO(9:1)/MWCNTs			18wt%	10.00wt%	2wt%	0.83wt%
ITO(1:1)/MWCNTs			10wt%	9.33wt%	10wt%	1.84wt%
In_2O_3/MWCNTs (Impregnation)			20wt%	16.07wt%		
In_2O_3/MWCNTs ($NaBH_4$)			20wt%	21.71wt%		
Pd/In_2O_3/MWCNTs (Impregnation)	20wt%	19.38wt%	16wt%	12.76wt%		
Pd/In_2O_3/MWCNTs ($NaBH_4$)	20wt%	18.86wt%	16wt%	15.97wt%		
Pd/SnO_2/MWCNTs	20wt%	18.30wt%			16wt%	1.08wt%

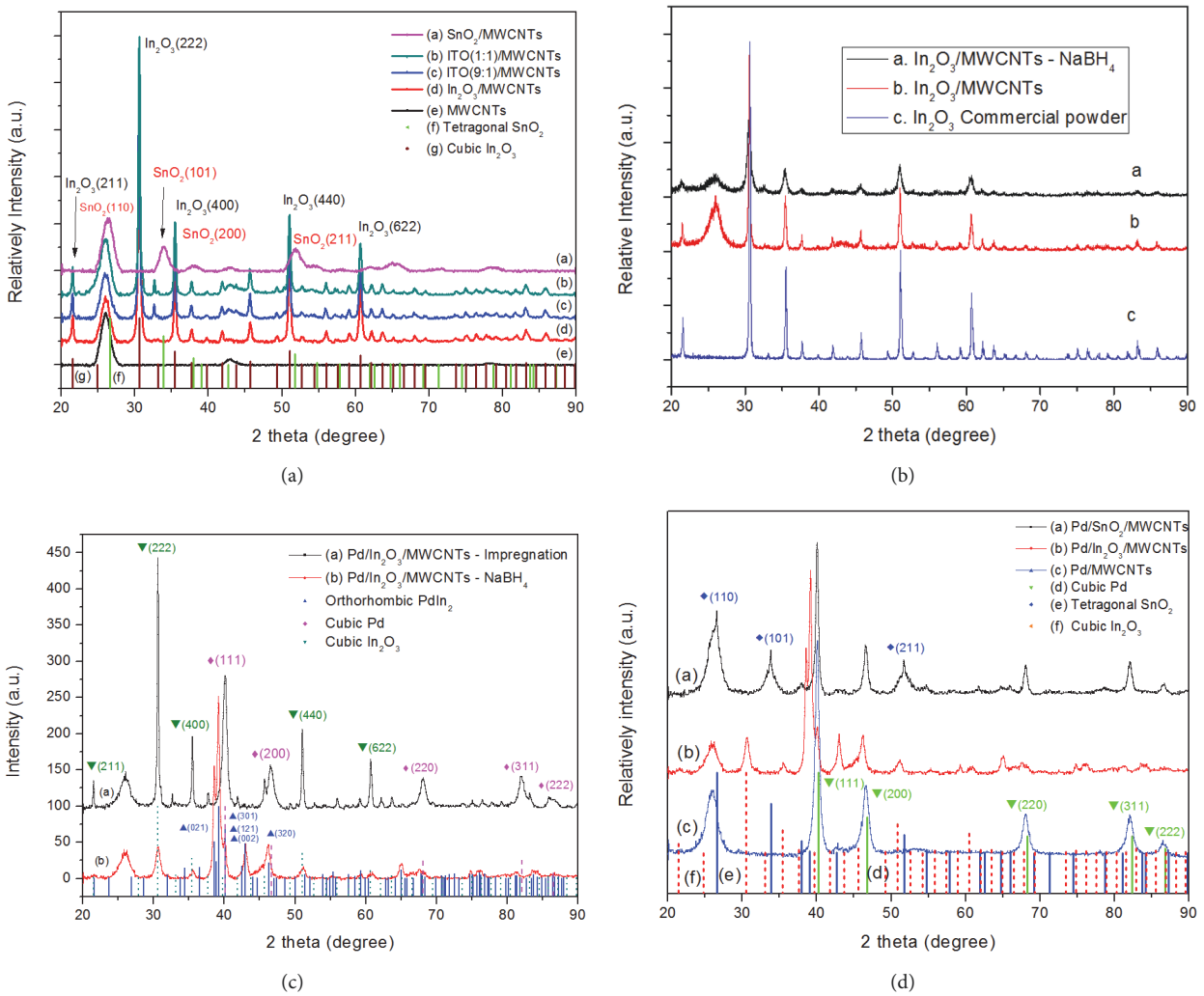

Figure 3: XRD patterns of the hybrid nanoparticles.

Table 2: The maximum current density and the corresponding potential of the prepared Pd based electrocatalysts.

	Pd/MWCNTs		Pd/In_2O_3/MWCNTs ($NaBH_4$)		Pd/SnO_2/MWCNTs		Pd/In_2O_3/MWCNTs (IM)	
	mV	mA/mg	mV	mA/mg	mV	mA/mg	mV	mA/mg
10	358	274.54	212	18.76	248	123.36	375	253.15
20	382	240.01	384	305.36	236	112.76	393	334.57
30	382	204.64	412	449.03	222	92.84	463	457.79
40	374	170.04	374	396.02	212	78.78	409	433.02
50	339	135.05	339	305.57	197	62.37	378	383.90
60	321	106.95	305	216.09	191	47.61	356	339.53

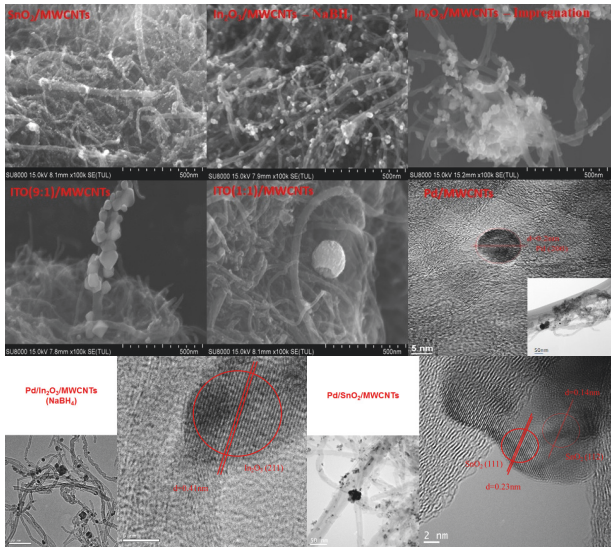

Figure 4: FESEM and HRTEM images of MOS/MWCNTs and Pd on various substrates.

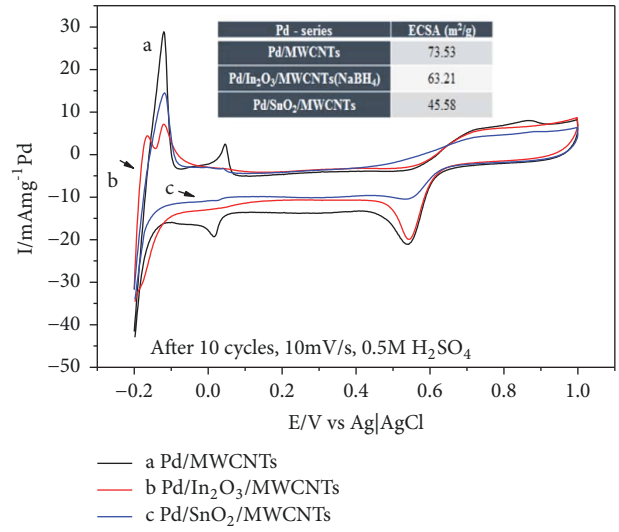

Figure 5: ECSA plots of the catalysts normalized by Pd weight.

similar Pd amount about 18-19 wt%. It reveals that Pd can be deposited on the surfaces of MWCNTs or metal oxides modified MWCNTs. For the two ITO mentioned previously, SnO_2 amounts are considerably smaller than the theoretical values and, for this reason, in this study Pd has not been deposited on the two ITO/MWCNTs. Pd/SnO_2/MWCNTs also have smaller SnO_2 amount than the theoretical value. The effect of SnO_2 in Pd/SnO_2/MWCNTs may not be as pronounced as expected.

3.2. Electrocatalytic Activity. The electrochemical surface area (ECSA) of the prepared Pd based electrocatalysts was measured by integrating current of surface PdO reduction peak. As shown in Figure 5, Pd/MWCNTs catalyst has the largest peak which means it has the largest electrochemical area. The ECSA data are shown in Table 2. The tendency of the electrochemical area of the catalysts is quite consistent with that of the particle size. That is, the smaller Pd particles of Pd/MWCNTs have larger surface area, and so, more active sites than the other two catalysts.

The electrocatalytical performance of the catalysts in the mixture of formic acid and sulfuric acid is shown in Figure 6 in a typical CV plot of every 10 cycles. All the corresponding potential and current data are summarized in Table 2. The maximum current densities of formic acid oxidation for Pd/MWCNTs and Pd/SnO_2/MWCNTs electrocatalysts decay continuously. The two Pd/In_2O_3/MWCNTs catalysts are activated at the first 30 cycles, then the current decays. The two Pd/In_2O_3/MWCNTs catalysts perform better in formic acid electrooxidation than Pd/MWCNTs, although they have smaller ECSA area. While activities of the two In containing catalysts are comparable, the Pd/In_2O_3/MWCNTs-IM performs better. The two effects can be responsible for the observed activity sequence: conversion of the Pd catalyst into Pd_2In in Pd/In_2O_3/MWCNTs-$NaBH_4$ and higher In_2O_3 content in Pd/In_2O_3/MWCNTs-IM. It is interesting that alloying of Pd by In improves the catalytic activity; however, the presence of In_2O_3 in the support also increases catalytic activity in even larger degree, which causes that the Pd/In_2O_3/MWCNTs-IM catalyst is most active. Such a high activity may be explained by two phenomena: (i) In_2O_3, like other oxides, helps to oxidize the adsorbed intermediate species, according to the bifunctional mechanism, or (ii) metal-support interaction changes palladium electronic properties, and so, its specific activity.

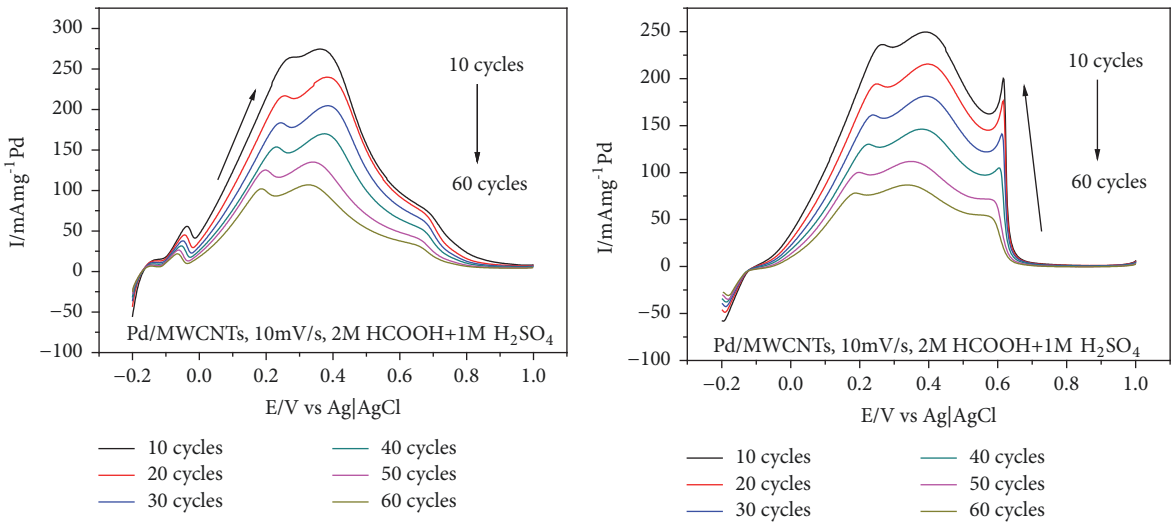

Figure 6: Pd/MWCNTs CV plot.

4. Conclusions

The MOS modified MWCNTs, SnO_2/MWCNTs, and In_2O_3/MWCNTs were successfully synthesized by the impregnation method. In_2O_3/MWCNTs was also prepared by $NaBH_4$ method and during the Pd deposition on this support by polyol method, the $InPd_2$ was formed. From FESEM and HRTEM images, it is seen that the fine Pd nanoparticles (around 2-10 nm) were deposited on the surface of MWCNTs and MOS/MWCNTs. The SnO_2 has the smallest particles (around 2-10 nm) comparing to other MOS particles and it uniformly dispersed on the surface of MWCNTs.

In electrochemical analysis of Pd-series catalysts, Pd/In_2O_3/MWCNTs catalyst, with In_2O_3 deposited by impregnation method, has the highest electrooxidizing current density in cyclic voltammetry experiments. Both ECSA and CV results indicate the Pd/In_2O_3/MWCNTs have the highest electrocatalytic activity. In the present results, In_2O_3 nanoparticle is the best electrocatalysts supporter in this study.

Data Availability

The data used to support the findings of this study are available from the corresponding author upon request.

Conflicts of Interest

The authors declare that they have no conflicts of interest.

Acknowledgments

The authors gratefully acknowledge the years grants (MOST 106-2221-E-036-021 and MOST 105-2221-E-036 -017 -MY2) from Taiwan Ministry of Science and Technology.

References

[1] X. Yu and P. G. Pickup, "Recent advances in direct formic acid fuel cells (DFAFC)," *Journal of Power Sources*, vol. 182, no. 1, pp. 124–132, 2008.

[2] X. Wang, J.-M. Hu, and I.-M. Hsing, "Electrochemical investigation of formic acid electro-oxidation and its crossover through a Nafion® membrane," *Journal of Electroanalytical Chemistry*, vol. 562, no. 1, pp. 73–80, 2004.

[3] S. Uhm, M. Seo, and J. Lee, "Competitiveness of formic acid fuel cells: In comparison with methanol," *Applied Chemistry for Engineering*, vol. 27, no. 2, pp. 123–127, 2016.

[4] K. Jiang, H. Zhang, S. Zou, and W. Cai, "Electrocatalysis of formic acid on palladium and platinum surfaces: from fundamental mechanisms to fuel cell applications," *Physical Chemistry Chemical Physics*, vol. 16, no. 38, pp. 20360–20376, 2014.

[5] N. V. Rees and R. G. Compton, "Sustainable energy: a review of formic acid electrochemical fuel cells," *Journal of Solid State Electrochemistry*, vol. 15, pp. 2095–2100, 2011.

[6] L. Zhang, Q. Chang, H. Chen, and M. Shao, "Recent advances in palladium-based electrocatalysts for fuel cell reactions and hydrogen evolution reaction," *Nano Energy*, vol. 29, pp. 198–219, 2016.

[7] S. O. Mert and A. Reis, "Exergoeconomic analysis of a direct formic acid fuel cell system," *International Journal of Hydrogen Energy*, vol. 41, no. 4, pp. 2981–2986, 2016.

[8] S. Z. Rejal, M. S. Masdar, and S. K. Kamarudin, "A parametric study of the direct formic acid fuel cell (DFAFC) performance and fuel crossover," *International Journal of Hydrogen Energy*, vol. 39, no. 19, pp. 10267–10274, 2014.

[9] W. L. Law, A. M. Platt, P. D. Wimalaratne, and S. L. Blair, "Effect of Organic Impurities on the Performance of Direct Formic Acid Fuel Cells," *Journal of The Electrochemical Society*, vol. 156, no. 5, p. B553, 2009.

[10] X. Yu and P. G. Pickup, "Novel Pd-Pb/C bimetallic catalysts for direct formic acid fuel cells," *Journal of Power Sources*, vol. 192, no. 2, pp. 279–284, 2009.

[11] X. Yu and P. G. Pickup, "Deactivation resistant PdSb/C catalysts for direct formic acid fuel cells," *Electrochemistry Communications*, vol. 12, no. 6, pp. 800–803, 2010.

[12] A. Mikołajczuk, A. Borodzinski, P. Kedzierzawski, L. Stobinski, B. Mierzwa, and R. Dziura, "Deactivation of carbon supported palladium catalyst in direct formic acid fuel cell," *Applied Surface Science*, vol. 257, no. 19, pp. 8211–8214, 2011.

[13] X. Yu and P. G. Pickup, "Deactivation/reactivation of a Pd/C catalyst in a direct formic acid fuel cell (DFAFC): Use of array membrane electrode assemblies," *Journal of Power Sources*, vol. 187, no. 2, pp. 493–499, 2009.

[14] H.-X. Zhang, S.-H. Wang, K. Jiang, T. André, and W.-B. Cai, "In situ spectroscopic investigation of CO accumulation and poisoning on Pd black surfaces in concentrated HCOOH," *Journal of Power Sources*, vol. 199, pp. 165–169, 2012.

[15] Y. Zhou, J. Liu, J. Ye et al., "Poisoning and regeneration of Pd catalyst in direct formic acid fuel cell," *Electrochimica Acta*, vol. 55, no. 17, pp. 5024–5027, 2010.

[16] P. Kedzierzawski, A. Mikołajczuk, A. Borodziński, B. Mierzwa, and L. Stobinski, "Novel metastable Pd-Ru catalysts for electrooxidation of formic acid," *ECS Transactions*, vol. 28, pp. 23–31, 2010.

[17] M. Wei, C. Hsu, and F. Liu, "One-pot synthesis of mixed-phase Pd-Ru/C as efficient catalysts for electro-oxidation of formic acid," *International Journal of Electrochemical Science*, vol. 11, pp. 2185–2196, 2016, http://www.electrochemsci.org/papers/vol11/110302185.pdf.

[18] D. Wu, M. Cao, M. Shen, and R. Cao, "Sub-5 nm Pd-Ru nanoparticle alloys as efficient catalysts for formic acid electrooxidation," *ChemCatChem*, vol. 6, no. 6, pp. 1731–1736, 2014.

[19] E. A. Baranova, N. Miles, P. H. J. Mercier, Y. Le Page, and B. Patarachao, "Formic acid electro-oxidation on carbon supported PdxPt1-x ($0 \geq x \geq 1$) nanoparticles synthesized via modified polyol method," *Electrochimica Acta*, vol. 55, no. 27, pp. 8182–8188, 2010.

[20] B. D. Adams, R. M. Asmussen, C. K. Ostrom, and A. Chen, "Synthesis and comparative study of nanoporous palladium-based bimetallic catalysts for formic acid oxidation," *The Journal of Physical Chemistry C*, vol. 118, no. 51, pp. 29903–29910, 2014.

[21] J. Chen, Y. Li, Z. Gao et al., "Ultrahigh activity of Pd decorated Ir/C catalyst for formic acid electro-oxidation," *Electrochemistry Communications*, vol. 37, pp. 24–27, 2013.

[22] Y. Hao, J. Shen, X. Wang et al., "Facile preparation of PdIr alloy nano-electrocatalysts supported on carbon nanotubes, and their enhanced performance in the electro-oxidation of formic acid," *International Journal of Hydrogen Energy*, vol. 41, no. 4, pp. 3015–3022, 2016.

[23] J. Chen, G. Wang, X. Wang, J. Tian, S. Zhu, and R. Wang, "Enhanced formic acid electro-oxidation on PdIr nanoparticles prepared by ethylene glycol-assisted NaBH4 reduction process," *Journal of Nanoscience and Nanotechnology*, vol. 13, no. 10, pp. 7008–7011, 2013.

[24] J. Wang, Y. Kang, H. Yang, and W. Cai, "Boron-Doped Palladium Nanoparticles on Carbon Black as a Superior Catalyst for Formic Acid Electro-oxidation," *The Journal of Physical Chemistry C*, vol. 113, no. 19, pp. 8366–8372, 2009.

[25] K. Jiang, J. Chang, H. Wang et al., "Small Addition of Boron in Palladium Catalyst, Big Improvement in Fuel Cell's Performance: What May Interfacial Spectroelectrochemistry Tell?" *ACS Applied Materials & Interfaces*, vol. 8, no. 11, pp. 7133–7138, 2016.

[26] H.-M. Kung, Y.-J. Chiou, H.-M. Lin, A. Borodzinski, L. Stobinski, and C.-K. Lin, "Anode catalyst of hybrid AuPd and rare earth doped cerium oxide/multi-walled carbon nanotubes for direct formic acid fuel cells," *Journal of the Japan Society of Powder and Powder Metallurgy*, vol. 63, no. 7, pp. 706–713, 2016.

[27] Y.-Y. Feng, Q.-Y. Yin, G.-P. Lu et al., "Enhanced catalytic performance of Pd catalyst for formic acid electrooxidation in ionic liquid aqueous solution," *Journal of Power Sources*, vol. 272, pp. 606–613, 2014.

[28] S. Takenaka, T. Tsukamoto, H. Matsune, and M. Kishida, "Carbon nanotube-supported Pd-Co catalysts covered with silica layers as active and stable cathode catalysts for polymer electrolyte fuel cells," *Catalysis Science & Technology*, vol. 3, no. 10, pp. 2723–2731, 2013.

[29] H. Xu, B. Yan, K. Zhang et al., "N-doped graphene-supported binary PdBi networks for formic acid oxidation," *Applied Surface Science*, vol. 416, pp. 191–199, 2017.

[30] S. Uhm, H. J. Lee, and J. Lee, "Understanding underlying processes in formic acid fuel cells," *Phys. Chem. Chem. Phys*, vol. 11, pp. 9326–9336, 2009.

[31] A. Boronat-Gonza, E. Herrero, and J. M. Feliu, "Fundamental aspects of HCOOH oxidation at platinum single crystal surfaces with basal orientations and modified by irreversibly adsorbed adatoms," *Journal Solid State Electrochem*, pp. 1–13, 2013.

[32] F. J. Vidal-Iglesias, A. López-Cudero, J. Solla-Gullón, and J. M. Feliu, "Towards more active and stable electrocatalysts for formic acid electrooxidation: antimony-decorated octahedral platinum nanoparticles," *Angew. Chem., Int. Ed*, vol. 52, pp. 964–967, 2013.

[33] J. Matos, A. Borodzinski, A. M. Zychora et al., "Direct formic acid fuel cells on Pd catalysts supported on hybrid TiO2-C materials," *Applied Catalysis B: Environmental*, vol. 163, pp. 167–178, 2015.

[34] Y.-J. Chiou, C.-D. Lu, H.-M. Lin, A. Borodzinski, L. Stobinski, and C.-K. Lin, "Synthesis and Characterization of Nano-hybrid Noble Metals/N doped TiO2/MWCNTs Electrocatalysts," *International Journal of Chemical Engineering*, vol. 2, pp. 68–72, 2015.

[35] R. Li, H. Hao, T. Huang, and A. Yu, "Electrodeposited Pd-MoOx catalysts with enhanced catalytic activity for formic acid electrooxidation," *Electrochimica Acta*, vol. 76, pp. 292–299, 2012.

[36] W.-L. Qu, D.-M. Gu, Z.-B. Wang, and J.-J. Zhang, "High stability and high activity Pd/ITO-CNTs electrocatalyst for direct formic acid fuel cell," *Electrochimica Acta*, vol. 137, pp. 676–684, 2014.

[37] A. Malolepszy, M. Mazurkiewicz, L. Stobinski et al., "Deactivation resistant Pd-ZrO2 supported on multiwall carbon nanotubes catalyst for direct formic acid fuel cells," *International Journal of Hydrogen Energy*, vol. 40, no. 46, pp. 16724–16733, 2015.

[38] H. An, H. Cui, D. Zhou et al., "Synthesis and performance of Pd/SnO2-TiO2/MWCNT catalysts for direct formic acid fuel cell application," *Electrochimica Acta*, vol. 92, pp. 176–182, 2013.

[39] L. Feng, J. Yang, Y. Hu, J. Zhu, C. Liu, and W. Xing, "Electrocatalytic properties of PdCeOx/C anodic catalyst for formic acid electrooxidation," *International Journal of Hydrogen Energy*, vol. 37, no. 6, pp. 4812–4818, 2012.

[40] J. Chang, L. Feng, C. Liu, W. Xing, and X. Hu, "An Effective Pd–Ni2P/C Anode Catalyst for Direct Formic Acid Fuel Cells," *Angewandte Chemie International Edition*, vol. 53, pp. 122–126, 2014.

[41] L. Feng, J. Chang, K. Jiang et al., "Nanostructured palladium catalyst poisoning depressed by cobalt phosphide in the electrooxidation of formic acid for fuel cells," *Nano Energy*, vol. 30, pp. 355–361, 2016.

[42] Y.-J. Chiou, M.-Y. Chung, H.-M. Lin et al., "Characterization of PANI-MWCNTs Supported Nano Hybrid Electrocatalysts," *Journal of Materials Science and Engineering*, vol. 7, no. 1-8, 2017.

[43] B. Lesiak, M. Mazurkiewicz, A. Malolepszy et al., "Effect of the Pd/MWCNTs anode catalysts preparation methods on their morphology and activity in a direct formic acid fuel cell," *Applied Surface Science*, vol. 387, pp. 929–937, 2016.

[44] M. Jin, H. Zhang, Z. Xie, and Y. Xia, "Palladium nanocrystals enclosed by {100} and {111} facets in controlled proportions and their catalytic activities for formic acid oxidation," *Energy Environ. Sci*, vol. 5, pp. 6352–6357, 2012.

[45] M. S. Masdar, N. Ngah, N. Mohamed Aslam, D. Panuh, S. K. Kamarudin, and W. R. W. Daud, "Effects of fuel concentrations, catalyst loadings and activation on the performance of direct formic acid fuel cell (DFAFC) stack," *Malaysian Journal of Analytical Sciences*, vol. 20, no. 4, pp. 877–884, 2016.

[46] S. Sharma and B. G. Pollet, "Support materials for PEMFC and DMFC electrocatalysts—a review," *Journal of Power Sources*, vol. 208, pp. 96–119, 2012.

[47] H. Yong and G. Changfa, "Carbon Nanotubes and Carbon Nanotubes/Metal Oxide Heterostructures: Synthesis, Characterization and Electrochemical Property," in *Carbon Nanotubes - Growth and Applications*, M. Naraghi, Ed., 2011.

[48] Y.-J. Chiou, K.-Y. Chen, H.-M. Lin et al., "Electrocatalytic properties of hybrid palladium-gold/multi-walled carbon nanotube materials in fuel cell applications," *Physical Status Solidi A*, vol. 208, no. 8, pp. 1778–1782, 2011.

[49] X. Zhang, H. Zhu, Z. Guo, Y. Wei, and F. Wang, "Sulfated SnO2 modified multi-walled carbon nanotubes - A mixed proton-electron conducting support for Pt catalysts in direct ethanol fuel cells," *Journal of Power Sources*, vol. 196, no. 6, pp. 3048–3053, 2011.

[50] W.-C. Chang, C.-H. Kuo, C.-C. Juan, P.-J. Lee, Y.-L. Chueh, and S.-J. Lin, "Sn-doped In2O3 nanowires: Enhancement of electrical field emission by a selective area growth," *Nanoscale Research Letters*, vol. 7, no. 1, pp. 1–7, 2012.

[51] N. Preissler, O. Bierwagen, A. T. Ramu, and J. S. Speck, "Electrical transport, electrothermal transport, and effective electron mass in single-crystalline In2O3 films," *Physical Review B: Condensed Matter and Materials Physics*, vol. 88, no. 8, 2013.

[52] J. Parrondo, R. Santhanam, F. Mijangos, and B. Rambabu, "Electrocatalytic performance of In2O3-supported Pt/C nanoparticles for ethanol electro-oxidation in direct ethanol fuel cells," *International Journal of Electrochemical Science*, vol. 5, no. 9, pp. 1342–1354, 2010.

[53] B. G. Pollet, "The use of ultrasound for the fabrication of fuel cell materials," *International Journal of Hydrogen Energy*, vol. 35, no. 21, pp. 11986–12004, 2010.

[54] B. G. Pollet and J. T. E. Goh, "The importance of ultrasonic parameters in the preparation of fuel cell catalyst inks," *Electrochimica Acta*, vol. 128, pp. 292–303, 2014.

[55] B. G. Pollet, "Let's Not Ignore the Ultrasonic Effects on the Preparation of Fuel Cell Materials," *Electrocatalysis*, vol. 5, no. 4, pp. 330–343, 2014.

[56] M. A. Matin, J.-H. Jang, E. Lee, and Y.-U. Kwon, "Sonochemical synthesis of Pt-doped Pd nanoparticles with enhanced electrocatalytic activity for formic acid oxidation reaction," *Journal of Applied Electrochemistry*, vol. 42, no. 10, pp. 827–832, 2012.

[57] J. Chen, Y. Li, S. Liu et al., "Remarkable activity of PdIr nanoparticles supported on the surface of carbon nanotubes pretreated via a sonochemical process for formic acid electrooxidation," *Applied Surface Science*, vol. 287, pp. 457–460, 2013.